Version of Record: https://www.sciencedirect.com/science/article/pii/S0038092X18308582
Manuscript_b460839f1a04a048c5b200b578f2d544

Deploying Effectively Dispatchable PV on Reservoirs: Comparing Floating PV to Other Renewable Technologies

Marc Perez[a], Richard Perez[b], Craig R. Ferguson[b] & James Schlemmer[b]

[a] Clean Power Research, Napa, CA, USA

[b] Atmospheric Sciences Research Center, University at Albany, SUNY, Albany, NY, USA.

ABSTRACT

In this article, we present a detailed simulation of floating PV's energy yield and associated evaporation reduction potential for the largest 128 US hydropower reservoirs. A recent article by Cavusoglu et al., published in the journal *Nature Communications*, outlined a hypothetical evaporation engine that could harness the energy of lake water evaporation while simultaneously conserving the water resource. Its authors suggested that evaporation engines deployed across all US lakes and reservoirs could, collectively, yield up to 70% of the total U.S. electricity production. We show that floating photovoltaic (PV) technology could: (1) deliver considerably more electrical energy than evaporation engines, amounting to 100% of the US production with only a fraction of the lakes; (2) deliver this energy on a firm, effectively dispatchable basis; and (3) conserve as much water as the evaporation engines.

1. Background

A new study by Cavusoglu et al. in Nature Communications[1] claims that deploying evaporation-driven electrical energy generators upon all US lakes could meet a sizeable fraction of the US demand for electrical energy. This new technology to turn water evaporation into energy is still at a very early pre-prototyping stage[2-10]. Its cost, operational reliability, and environmental impact have yet to be established.

We aim to demonstrate that, if one were to seriously consider using lakes for energy technology deployment, PV would be considerably more effective than evaporation technology. PV could produce the same quantity of electricity and cost-optimally deliver this electricity with firm (24/7) production guaranties, while occupying only a small fraction of available lake area – specifically, only a fraction of managed reservoirs – and provide equivalent water conservation potential.

Through our systematic quantification of the electrical power generation potential and the water conservation potential of floating PV for the largest US reservoirs, we develop clear, new, actionable information for industry and decision-makers to better assess lake deployment options. In addition to a comparison with evaporation engine potential, we also contrast the floating PV potential to the current hydropower production potential of the reservoirs.

© 2018 published by Elsevier. This manuscript is made available under the Elsevier user license
https://www.elsevier.com/open-access/userlicense/1.0/

2. Assumptions and methods

2.1 U.S. reservoir characteristics

As quantitative support for our investigation, we consider the 128 largest US reservoirs with a full lake storage capacity of one km^3 and above. Many of these reservoirs are exploited for the production of electricity via hydropower. A table is provided in the Appendix including the reservoirs' physical characteristics and their current hydropower generation specifications. This reservoir sample amounts to about 30% of the area of the water bodies considered in Cavusoglu et al. (2017) [1].

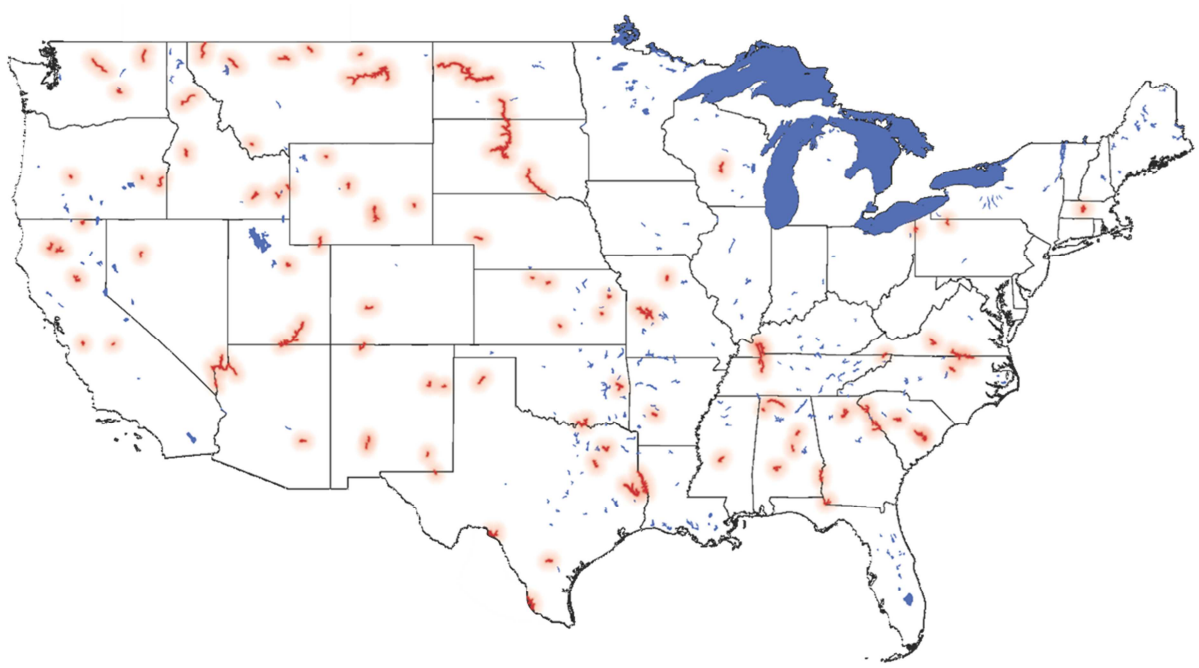

Figure 1: US lakes and reservoirs – the 128-reservoir sample used in this study is highlighted in red.

2.2 Photovoltaic (PV) efficiency

We assume that the highest achieved module efficiency of 24% for commercial grade crystalline silicon photovoltaic modules[14], while it is cutting-edge today, will represent conservative mainstream conditions in the near future. This assumption is reasonable for the long-term, large scale deployment planning implied in this paper.

2.3 PV array configuration

We assume that floating PV arrays are stationary and tilted southward at 10^o. This geometry is sub-optimal from an energy production standpoint per unit of collector area[15]; however, it is nearly ideal from a ground [lake] energy density standpoint. Allowing 15-20% spacing to account for maintenance and [minimal] row-shading considerations, the footprint conversion efficiency of the installed arrays

thus reaches roughly 20% (i.e., 24% minus the non-PV areas). This amounts to a peak power density of 200 W/m^2 (at 1000 W/m^2 incoming irradiance) of ground [lake] area under standard test conditions[16].

2.4 Floating PV technology

The floating PV industry is new but it is fast developing. While it is still experiencing design complexity and cost issues at this stage of its learning curve[17] , multiple medium-to-large commercial-scale projects are already currently operational [18, 19]. These projects totaled several hundred MWs as of early 2018.

The possible benefits of floating PV are multiple and echoed in numerous publications on the subject[20-23]. Floating PV has been implemented in locations with a favorable tradeoff compared to land-based deployment, taking advantage of available and unexploited areas (wastewater basins, for instance). It can reduce evaporation, algae growth, the formation of waves and coupled erosion effects. Moreover, it can increase hydropower resource availability via evaporation reduction. Furthermore, the floating structural elements may serve important secondary functions, such as storage for compressed air. The vast potential for floating PV was perhaps most recently demonstrated for China. Liu et al.[24] estimated the potential for floating PV at 160 GW with 2% lake coverage and 8000 GW—enough capacity to generate China's (2015) annual electrical demand—with full lake coverage.

Undeniably, floating PV has drawbacks that need to be carefully taken into consideration, including aesthetics, loss of recreational use, and water quality issues (e.g., temperature) that could affect ecosystems. Nevertheless, in the context of this paper, these potential drawbacks are not different from the evaporation engine technology's against which floating PV is contrasted, and likely, less impactful, especially from an aesthetics standpoint.

Figure 2: 70 MW Floating PV plant on a clay quarry lake in Anhui Province, China under construction by Ciel & Terre (source: Ciel & Terre)

2.5 Mean PV electrical energy production density

A peak output of 200 W/m^2 of ground [lake] surface amounts to a mean output of 30-50 W/m^2 in the Contiguous U.S. (CONUS) depending on the local solar resource[25]. We contrast this number to a recent NREL study reporting a mean density of only 8 Watts per m^2 for typical utility-scale PV farms[26]. It is important to note that this NREL study surveyed existing terrestrial installations where ground density has not been a premium concern, and where module efficiency has been historically lower than what is achievable today. There is no physical or technical reason, given current and foreseeable PV technology, why [floating] low-tilt PV arrays could not yield 30-50 average W/m^2 mean power generation density or more in the future.

2.6 Firm PV electrical generation density

Firm power generation is the ability to meet a given electrical demand at all times. When considering conventional resources, firmness is achieved with baseload generation (chiefly nuclear, large hydro and coal) plus the *dispatching* of flexible generation (chiefly natural gas turbines) as needed for production to match demand.

PV generation is inherently intermittent, modulated by day-night cycles, weather, and seasonal effects. It cannot be dispatched by grid operators and cannot, by itself, meet demand at all times. Applying energy storage can render PV+storage fully dispatchable and transform PV into a firm power generation resource. However, applying storage alone to deliver firmness would be prohibitively expensive, even with the most optimistic storage technology cost projections. This is because in addition to supplying power at night, storage systems would also have to be large enough to make up for extended cloudy periods and seasonal deficits.

However recent work by the authors and others has shown that oversizing PV deployments and proactively curtailing output could deliver firm (365/24/7) electricity to regional power grids[27,28,29,30] at an acceptable production cost. This counter-intuitive approach of oversizing PV and dynamically curtailing output significantly reduces storage requirements to the point where total (PV+storage) system costs become considerably lower despite the oversizing of PV.

The relationship between the relative cost contributions of PV and storage to meet a baseload production target 100% of the time (i.e., the equivalent of a nuclear generating facility) is illustrated in Figure 3 for an example in the New York metro area. In this example, optimum production cost is achieved when oversizing PV by about two and curtailing half of the output. This *cost-optimized* PV-plus oversizing-plus storage-plus curtailment resource meets demand with 100% certainty. Hence, it is *effectively dispatchable*. While it may not be dispatchable in the traditional sense, it meets the central criterion of dispatchability: meeting load demand under any circumstance.

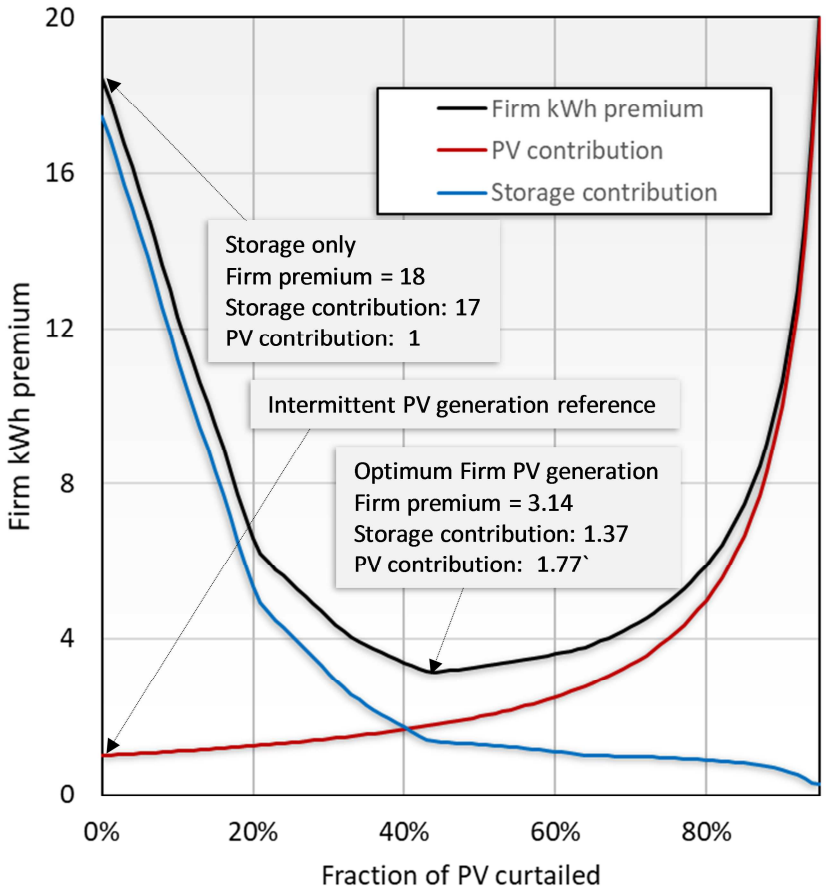

Figure 3: Influence of PV curtailment on firm PV generation cost in the northeastern US [29]. The y-axis represents the firm KWh premium in reference to unconstrained (i.e., intermittent) PV kWh. The x-axis represents the curtailed PV fraction.

An optimized blend of oversized PV and storage with proactive operational curtailment yields firm, on-demand power generation at production costs that are not as unrealistically high as applying storage alone. When coupled with other solutions such as geographical dispersion, demand-side load flexibility, or even adding an optimized wind-PV blend, an optimized overbuild/curtailment strategy could deliver firm 24/7 baseload production at costs well below 10 cents per kWh in a moderate solar resource State such as Minnesota [29]. This firm generation cost could approach 4-5 cents per kWh at the 25-year time horizon as PV and load-firming technologies continue their downward trend[31].

Authors observed that oversizing by a factor of about two yielded lowest-cost firm power generation capability. They noted that in addition to resource vs. load requirements, this optimum factor depended on the relative capital and operating costs of PV and storage. However, given foreseeable expected cost for storage and PV (the example in Figure 3 assumes future, achievable turnkey costs of respectively $1,000/kW for PV and $100/kWh for storage), a factor of about two was found to be near optimal in the Northeast US with slightly less oversizing needed in sunnier climates.

Therefore, using this oversizing of two estimate as a measure of lowest-cost firm PV generation, we introduce the term *Firm PV Production Density,* as one-half of the mean PV electrical energy production density. This *Firm PV Production Density* thus amounts to 15-25 Watts per m^2 with guaranties of cost-optimally meeting utility demand at all times.

2.7 Site-specific PV output modeling

We simulated hourly AC electricity production for each artificial reservoir for a period of ten years (2006-2015). In order to do so, we applied the operational SolarAnywhere[32] suite of models that combine intermediate-resolution (10 km, hourly) gridded satellite-derived irradiances from the SUNY model[33] and a PV simulation engine based on PVFORM/PVWATTS[34,35] to convert irradiance and meteorological data into PV electrical production. The SUNY radiation model exploits the shortwave and infrared channels of geostationary weather satellites to estimate site and time-specific cloud transmission that modulates simple clear-sky atmosphere radiative transfer models (these clear-sky models are themselves based upon operational aerosol optical depth, precipitable water, and atmospheric ozone data.) The SUNY model has been extensively validated, with observed long-term biases well below 3%[36] in the CONUS. The PV simulation engines, coupled with satellite-derived irradiances, are widely used by the solar and utility industries for feasibility studies and operational monitoring[37].

2.8. Site-specific reservoir evaporation estimates

Where deployed, floating PV eliminates the lake-atmosphere interface. Thus, to first order, water conservation amounts to the water that would otherwise have been lost to evaporation over the surface area occupied by floating PV. To calculate this time-varying and site-specific avoided evaporation, we applied the European Centre for Medium-Range Weather Forecasts (ECMWF) Integrated Forecasting System (IFS[38]) cycle 43r1 implementation of the Fresh-water Lake model (FLake[39]). FLake is comprised of a well-mixed surface layer with uniform temperature and a thermocline, which is bounded at the top by the mixed layer bottom and below by the lake bottom. FLake accounts for the following prognostic variables: mixed-layer temperature, mixed-layer depth, bottom temperature, and mean temperature of the water column, shape factor (of the temperature profile in the thermocline), lake ice temperature, and ice thickness. Despite its relative simplicity, FLake has proven skillful in prior intercomparisons[39]. Any snowpack on the lake is modeled by the IFS's land physics package, the Hydrology Tiled ECMWF Scheme of Surface Exchanges over Land (HTESSEL[41]) (ECMWF[38]).

In our study, each lake is modeled using a single representative grid. Each grid is initialized with prognostic temperatures set to 280K, a mixed-layer depth of 5m, shape factor of 0.65, and ice thickness of zero. A single external variable, lake depth, was prescribed according to simple geometric calculations based on the reservoir capacity and surface area estimates (Table A1). Deeper lakes tend to be less well-mixed and lose less water to evaporation on a per area basis compared with shallower lakes. To allow for the 'spin-up' of each lake, the FLake model was integrated for a full calendar year leading up to our 10-year analysis window (2006-2015).

Hourly meteorological inputs to FLake were taken from Princeton University's 4 km hourly meteorological forcing dataset (PUmet[44]). PUmet shortwave radiation is derived from the Geostationary Operational Environmental Satellite (GOES) surface Solar Insolation Product (GSIP) Level 2

product[45]. Other forcing fields are downscaled from the 0.125° North American Land Data Assimilation System Phase 2 (NLDAS-2[46,47]) dataset with adjustment for elevation and physical consistency[42]. The non-precipitation fields for NLDAS-2 are derived from the 3-hourly and 32 km analysis fields of the National Oceanic and Atmospheric Administration (NOAA) National Centers for Environmental Prediction (NCEP) North American Regional Reanalysis (NARR[48,49]).

Because its use is still prevalent in the hydrological modeling community[50], the Penman-Monteith (P-M) model[51,52] was applied with PUmet forcing to compute comparative lake water evaporation estimates. For our calculations, we assumed: a lake heat flux equal to 26% of net radiation[53], bulk surface resistance of 70 s m-1, shortwave albedo of 0.07, and momentum roughness of 0.0001m. The P-M approach yielded physically unrealistic instances of nighttime negative evaporation (i.e., condensation) over the lakes, which amounted on average to more than 8.7% of total evaporation. At nighttime, there should be no condensation because the lake surface will be warmer than the air advected from surrounding land, which sets-up an unstable atmospheric condition with evaporation. We chose to disregard all nighttime P-M estimates (negative or positive evaporation) because the model is not physically representative during that period and suggest this approach to the community. Generally speaking, P-M estimates of lake evaporation should be interpreted with caution.

Figure 4 compares the results of the two methodologies for the 128-reservoir sample. The P-M daytime estimates are 8.1% less on average and 10.1% less on median than those of FLake. FLake evaporation estimates exceed those of P-M daytime for all except ten reservoirs, including Strawberry Reservoir, UT (-28% or 13 mm yr^{-1}) and Flaming Gorge Reservoir, UT/WY (-16% or 10 mm yr^{-1})(Figure 7).

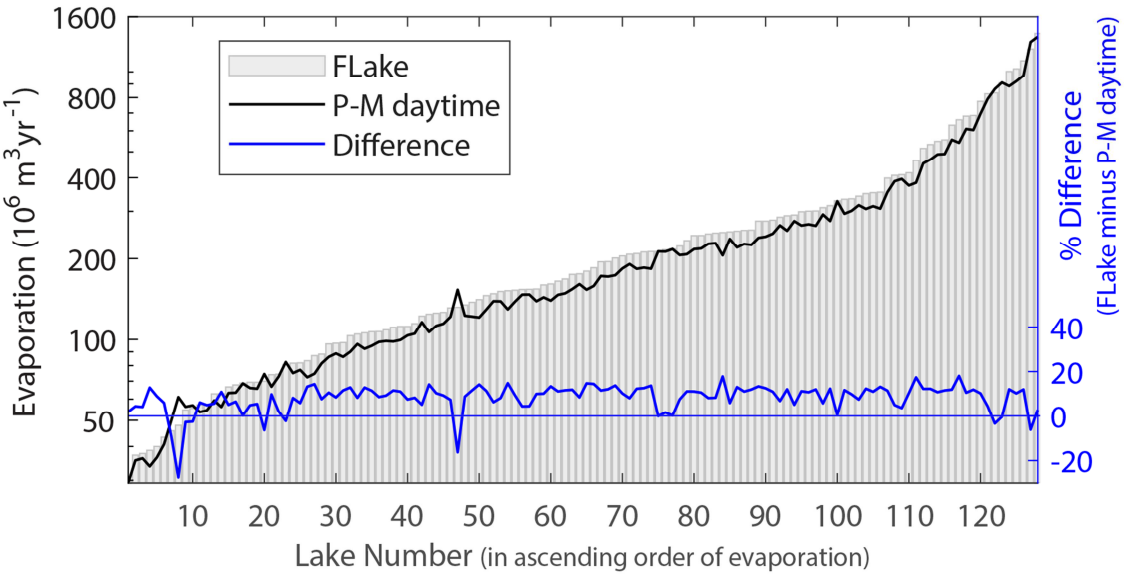

Figure 4: Comparing FLake and Penman-Monteith results for the 128-reservoir sample.

2.9 Comparison of PV, evaporation engine, and hydropower generation capacity

We quantify PV energy yield and evaporation reduction associated with the area covered by the floating PV using 10-years' worth of high-resolution solar resource and meteorological data. For the evaporation engine, we estimate the energy yield and water conservation for each reservoir from the statewide data published in Cavusoglu et al. (2017)[1]. That data includes annual energy yield, water conservation and total lake area for 15 US states. From this information, we infer reservoir-specific energy and water yields via interpolation/extrapolation of these statewide energy and water conservation densities. For hydropower, we apply a US-wide capacity factor of 40% to all reservoirs. For the last five years, mean US hydropower generation has averaged 40% of peak capacity [11]

3. Results

3.1 PV power generation

Mean annual photovoltaic (PV) electrical generation densities simulated for the selected 128-reservoirs are reported in figure 5 (top). These densities are a function of climate and range from 28 W/m^2 at Riffe Lake in Washington State to 48 W/m^2 at Elephant Butte Reservoir in New Mexico. Figure 5 (bottom) reports the mean power generation potential of each reservoir assuming 100% PV coverage over their full lake areal extent. Figure 5 also reports the existing peak hydropower generating capacity of the reservoirs that are so equipped (100 out of 128; see Appendix). Peak hydropower generation represents the maximum power output of the existing turbines.

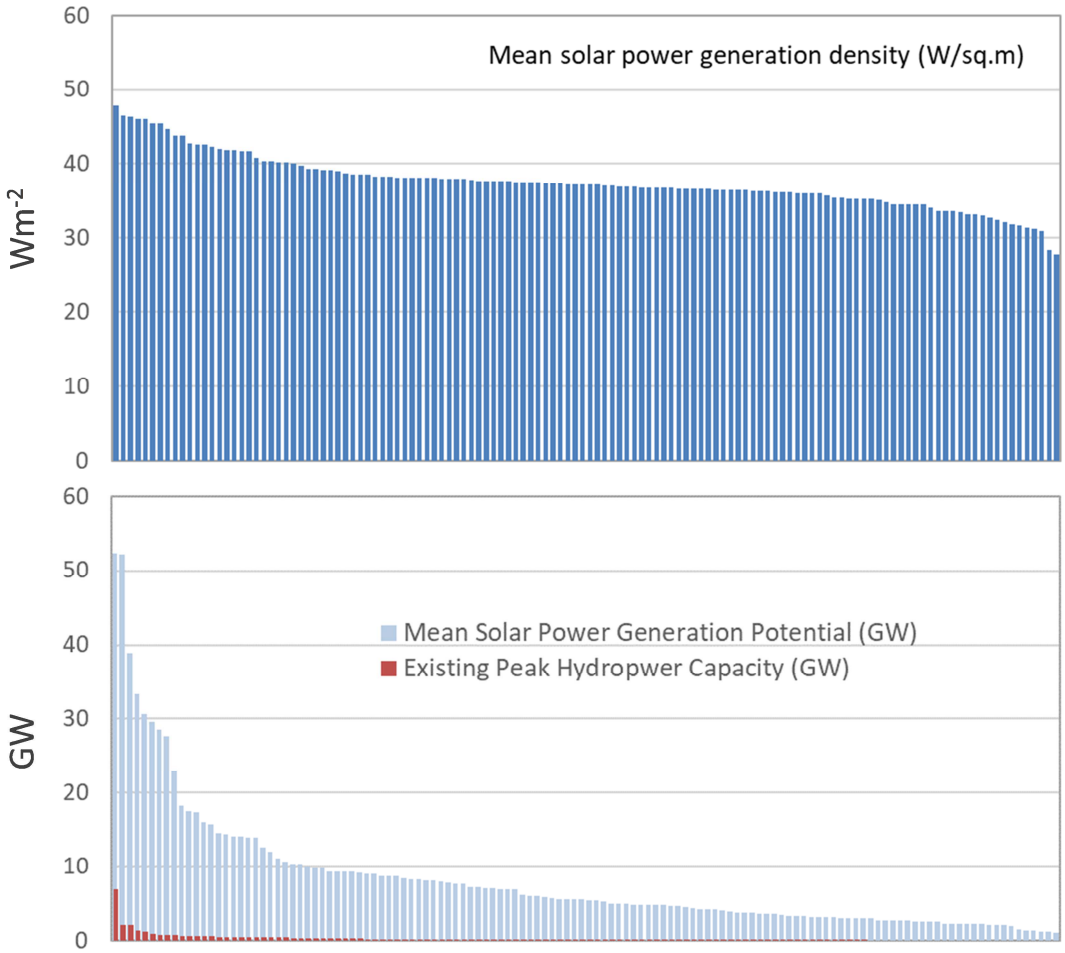

Figure 5: Sorted mean PV power densities for the 128 reservoir sample (top); and sorted mean lake-wide PV production (bottom) contrasted to current peak hydropower capacity.

The total potential PV generating capacity across all 128 reservoirs adds up to 1050 GW. This amounts to an annual electrical energy production of 9,250 TWh. By comparison, the total hydropower peak capacity for the considered lakes is 32 GW. Assuming a 40% capacity factor (see Section 2.9), the annual hydropower production is 112 TWh, or about 80 times less than potential PV generation assuming full coverage. Therefore, covering 1.2% of the reservoirs' surface area with floating PV would produce as much electricity as hydropower turbines currently produce.

3.2 Firm, effectively dispatchable PV power generation

With an oversizing factor of two and a proactive output curtailment of 50%, PV plants and associated enabling technologies (storage, grid strengthening and demand response) can cost-optimally meet utility demand with 100% certainty. The firm, guaranteed electricity generation capacity of PV for the 128-reservoir sample thus amounts to one-half of the mean PV generating capacity, i.e., 525 GW,

corresponding to an annual energy production of 4,620 TWh. This exceeds the 2016 US electricity consumption of 4,100 TWh[12].

3.3. Contrasting PV and evaporation technology

The evaporation technology study considered all inland water bodies in CONUS, both artificial and natural, excluding the Great Lakes. This represents a total area of 95,000 km^2. The study claims that covering this entire area with evaporation engines would deliver 325 GW electrical on average, which would fall somewhat short of firm power capability. Indeed, like PV, the evaporation engine technology is weather/climate driven—a function of local temperature, relative humidity and downwelling radiation. It does have built-in weather variability mitigation capability via heat storage in the underlying bodies of water that allows for some level of load following. However, this is not enough to guaranty firm power delivery everywhere without additional technologies (e.g., battery storage). While in some states with favorable evaporative conditions, firm demand-following could be achieved, in other states it would fall short of meeting demand at all times. In the state of New York, for instance, the authors indicate that the technology could only meet demand 67% of the time.

The reservoir sample considered here covers 29,000 km^2. For this area, the evaporative engine technology would deliver 100 GW on average, adding up to 880 TWh worth of electricity annually (firmly in some, but not all cases). This is considerably less than the firm PV potential of 4,620 TWh covering the same area. Interestingly, both technologies far exceed the current hydropower [firm] generation capability of 120 TWh/year. The yields of the three technologies are compared in Figure 6 for all reservoirs.

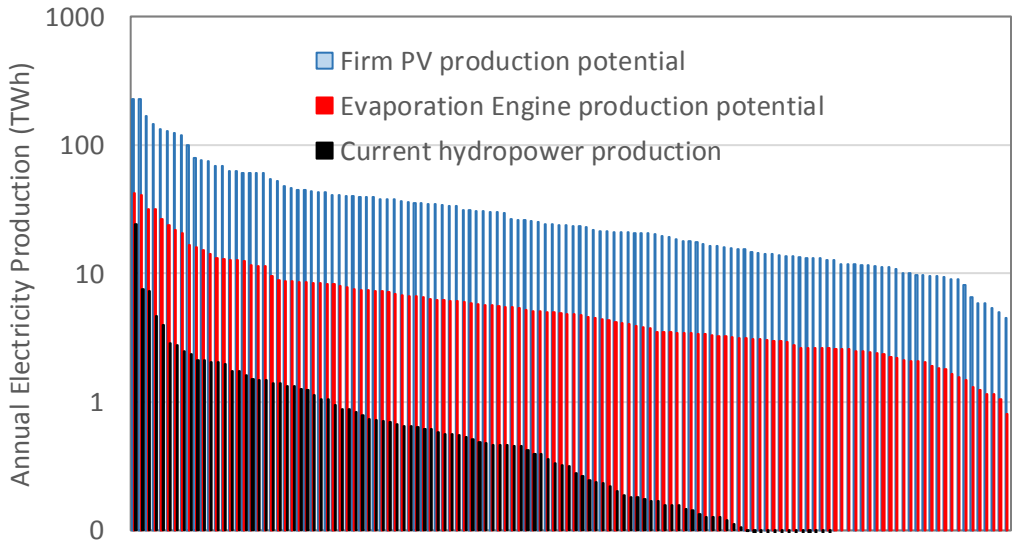

Figure 6: Contrasting floating PV and evaporation engine electricity generation potential to current hydropower production for the 128 reservoirs sample. Full reservoir coverage is assumed for both PV and evaporation engine

In Table 1, we compare the energy generation potential of PV and evaporation engines to the current electrical generation of selected states assuming equal lake surface coverage (i.e., all in-state water bodies).

TABLE 1: Comparing PV and evaporation engine electricity generation potential for 15 US states

	Cavusoglu et al., (2017) evaporation engines			This study 128-reservoirs PV production		PV production prorated to Cavusoglu et al., lake areas			
State	Considered lake area (km^2)	Potential power available with evaporation engines(MW)	Current state net electrical generation (MW)	Considered lake area km2	Mean power available from PV (MW)	Mean Power Available from PV (MW)	Firm Power Available from PV (MW)	Ratio to evaporative technology	Ratio to state Net generation
Utah	8,393	47,201	4,789	239	9,855	345,408	172,704	366%	3606%
California	4,845	27,551	22,455	657	27,202	200,654	100,327	364%	447%
Minnesota	8,996	19,252	6,505	1,859	61,731	298,774	149,387	776%	2297%
Louisiana	4,414	14,353	12,307	735	27,716	166,438	83,219	580%	676%
Nevada	1,710	12,292	4,457	757	33,263	75,156	37,578	306%	843%
Oklahoma	2,729	9,832	8,691	1,948	73,562	103,086	51,543	524%	593%
Oregon	2,383	8,994	6,606	432	15,584	85,961	42,980	478%	651%
Montana	2,854	8,628	3,345	2,058	67,999	94,322	47,161	547%	1410%
Maine*	4,029	8,358	1,340	99	3,241	131,540	65,770	787%	4907%
S.Dakota	3,031	7,617	1,100	640	22,724	107,569	53,784	706%	4891%
Idaho	1,817	6,897	1,788	805	28,063	63,305	31,653	459%	1770%
N.Dakota	2,832	6,834	4,242	3,050	104,484	97,012	48,506	710%	1144%
Wyoming	1,420	6,005	5,590	171	6,903	57,305	28,652	477%	513%
N.Mexico	599	3,735	3,733	196	9,286	28,372	14,186	380%	380%
Vermont*	1,247	2,776	226	99	3,241	40,703	20,351	733%	8995%

**Note: for Vermont and Maine we used Massachussets as a basis for proration, since our 128-lake sample does not include these states.*

On average for these states, the mean PV power generation potential is one order of magnitude (ten times) larger than the evaporative engine technology's mean power availability. When considering firm, effectively dispatchable PV generation capability, the ratio between the two approaches averages 5:1 across all states. Interestingly, but not unexpectedly, the relative advantage of PV over the evaporation engine is larger in colder cloudy/humid states (e.g., Minnesota, Maine) than in warmer/drier southwestern states (e.g., Nevada, New Mexico).

3.4 PV water conservation potential

Figure 7 (top) illustrates the annual water conservation densities achievable by PV deployment for each of the 128 considered reservoirs. As noted previously, water conservation density is assumed equal to the net evaporation per unit area and we do not model for potential feedback between PV-covered and uncovered surface fractions. Water conservation densities range from a maximum conservation density of 1850 millimeters per year at Falcon Lake, TX, to a minimum of 680 millimeters per year at Strawberry Reservoir, UT. Evaporation rates vary according to net available energy, air temperature, humidity, and

wind speed. For instance, Falcon Lake, at 26.7°N receives greater insolation and higher vapor pressure deficits and sustained winds than Strawberry Reservoir at 40.2°N. FLake-based estimates additionally account for the thermal inertia of the reservoirs.

The total annual water conservation achievable for the 128 reservoirs is plotted at the bottom of Figure 7. Across all considered reservoirs, total water conservation achievable assuming 100% coverage amounts to 28 cubic kilometers, i.e., more than the fresh water withdrawals of the State of Idaho and over half of California's.

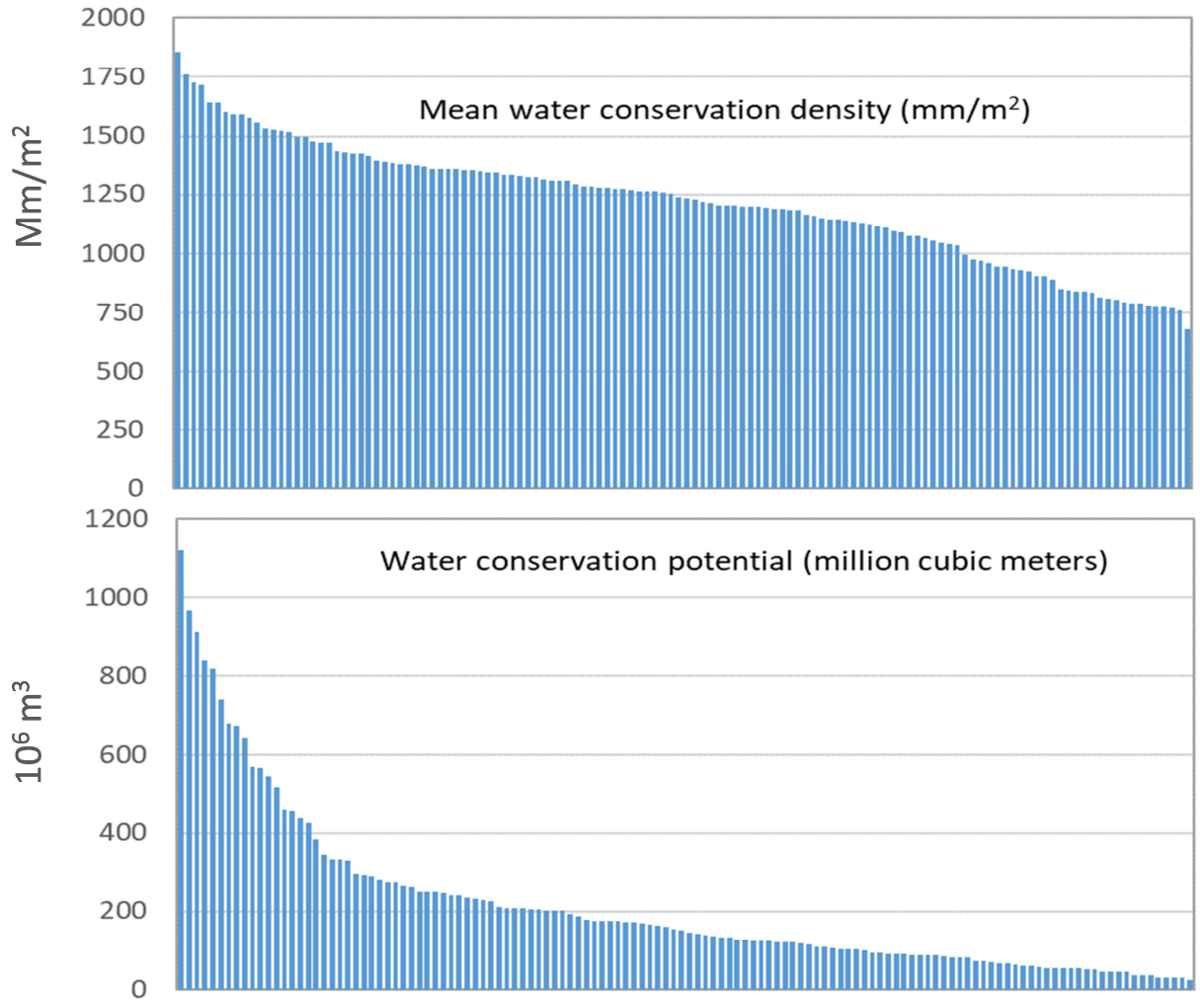

Figure 7: Sorted annual water conservation densities (top) and total annual water savings (bottom) for the 128-reservoir sample

The water conserved could be used to meet consumptive demands or to enhance hydropower potential, because water saved could also be fed to the turbine generators. This prospective hydropower generation enhancement is illustrated in Figure 8 compared to the existing mean power generation for each reservoir. The enhancement is not negligible, totaling 565 MW across all lakes, but only amounts to a small fraction (3%) of the existing hydropower resource. Relative to the generation potential of floating PV this secondary hydropower enhancement impact is almost insignificant (0.1%).

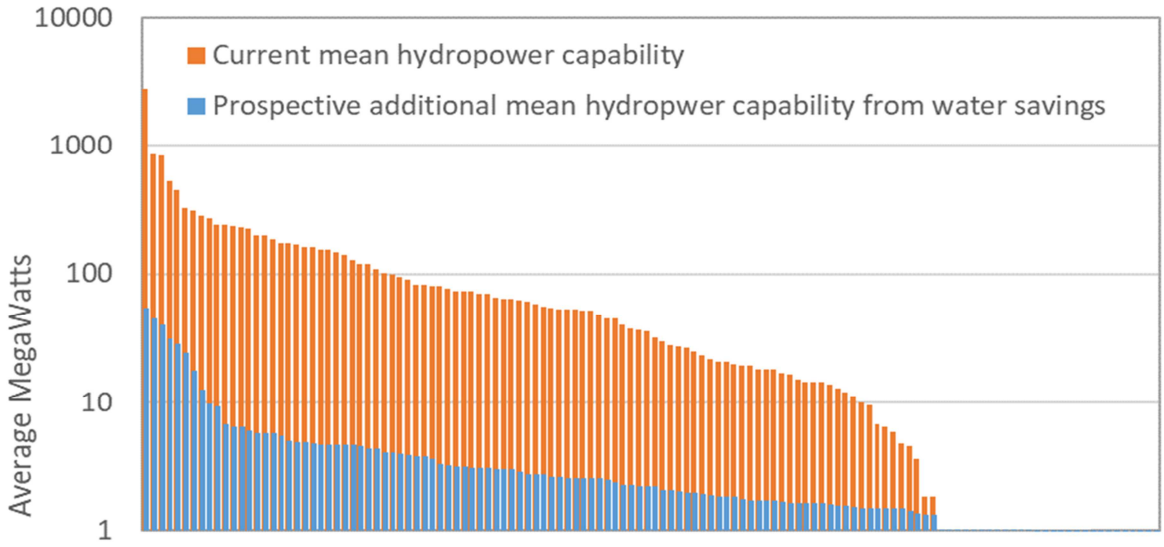

Figure 8: Comparing existing mean hydropower generating capacity and prospective additional capacity resulting from evaporation reduction for the 128-reservoir sample. (Note: only 101 reservoirs are currently equipped for power generation)

3.5. Contrasting PV and evaporation engine for water conservation

In Figure 9, we compare the water conservation potential of PV and evaporation technology for all reservoirs, assuming full coverage. As explained in the methods section, PV-induced conservation is computed from 10 years of site-specific irradiance and meteorological data, while lake-specific evaporation engine-induced conservation is inferred from published state-aggregated data[1].

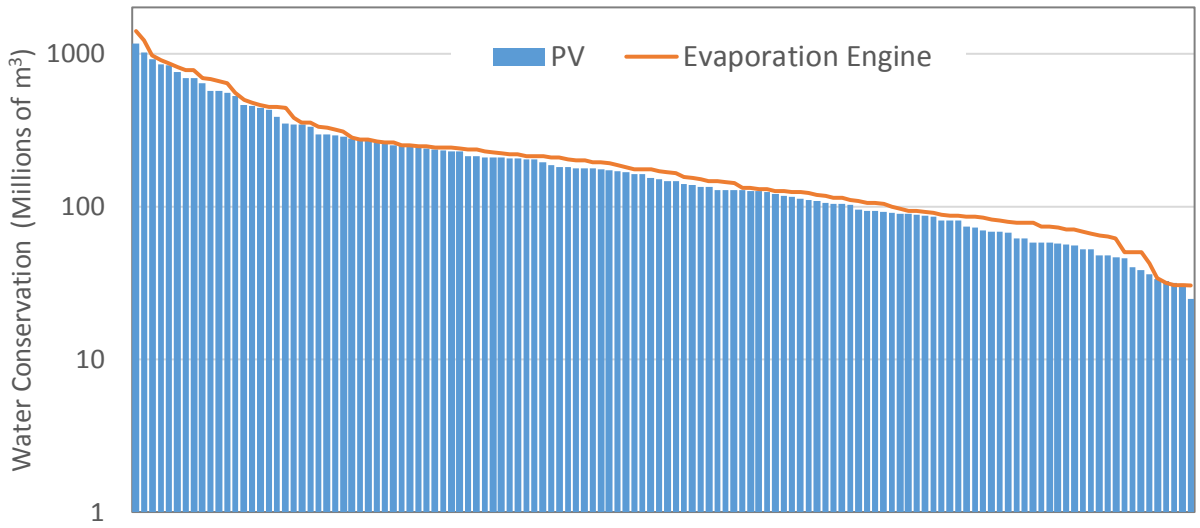

Figure 9: Comparing sorted PV and evaporation engine water conservation potential for all 128 reservoirs assuming full coverage. Evaporation engine conservation potential adapted from Cavusoglu et al. (2017) whereas floating PV conservation potential computed by FLake (see Section 2.8).

Given the difference between the two approaches in terms of modeling, site-specificity, data sources and time spans, the results between the two technologies are remarkably similar – less than 10% difference in overall water conservation potential. This similarity is not fortuitous because the underlying cause of water conservation is the same for both technology: evaporation suppression in the case of PV and conversion to energy in the case of the evaporation engine – both are proportional to the technology-covered area.

This similarity also confirms that the modeling approach applied in this article is sound. Small differences between our water savings estimates and those of Cavusoglu et al. (2017)[1] may be attributed to differences in evaporation models and meteorological data employed. Namely, we did not need to account for the energy conversion process of the conceptual evaporation engine. In addition, instead of a typical meteorological year dataset, we chose to use a 10-year real-time dataset with inherent interannual variability, and we applied a lake model to account for the important role of lake heat storage in evaporation.

In Table 2, we contrast statewide evaporation-engine water conservation potential to PV's. Both technologies lead to water conservation that exceeds statewide freshwater withdrawals[1] in some cases (e.g., Maine, the Dakotas and Oklahoma). However, it only amounts to a modest fraction of demand in states with intensive agricultural water use, such as Idaho and California.

TABLE 2: Comparing PV and evaporation engine water conservation potential for 15 US states.

	Cavusoglu et al., (2017) evaporation engines			This study 128-reservoirs PV production		PV production prorated to Cavusoglu et al. lake areas	
State	considered lake area (km^2)	Potential water savings 10^6 m^3/yr	State fresh water withdrawals 10^6 m^3/yr	considered lake area km2	Potential water savings 10^6 m^3/yr	Potential water savings 10^6 m^3/yr	Percentage of state withdrawals
Utah	8,393	10,541	5,711	239	141	4,943	87%
California	4,845	6,376	43,049	657	664	4,901	11%
Minnesota	8,996	6,651	5,279	1,859	1,172	5,673	107%
Louisiana	4,414	4,704	11,804	735	911	5,473	46%
Nevada	1,710	2,586	3,614	757	993	2,243	62%
Oklahoma	2,729	3,160	2,455	1,948	2,147	3,009	123%
Oregon	2,383	2,333	9,313	432	393	2,168	23%
Montana	2,854	2,615	10,546	2,058	1,403	1,945	18%
Maine*	4,029	2,845	565	99	72	2,934	519%
S.Dakota	3,031	2,762	865	640	503	2,379	275%
Idaho	1,817	1,795	23,806	805	563	1,269	5%
N.Dakota	2,832	2,425	1,567	3,050	2,087	1,938	124%
Wyoming	1,420	1,543	6,414	171	121	1,005	16%
N.Mexico	599	874	4,367	196	218	667	15%
Vermont*	1,247	1,019	596	99	72	908	152%

**Note: for Vermont and Maine we used Massachussets as a basis for proration, since our 128-lake sample does not include these states.*

4. Summary and Discussion

We have shown that, in terms of energy production, deploying floating PV on US lakes would be considerably more space-efficient than deploying a prospective evaporation-based technology. Deployed on the 128 largest US reservoirs floating PV could supply firm, 24/7 electricity equivalent to 100% of US electrical demand. Deployed on all the lakes considered for evaporation engine study, floating PV would produce 10 times that amount. In terms of water conservation, the floating PV potential is comparable to that of the evaporation engine's.

We also showed that PV is considerably more space-efficient than the hydroelectric power generation facilities currently operational at the considered reservoirs. Covering 1.2% of their surface with PV would generate as much electrical energy as hydropower currently generates. This finding may carry important prospects for water managers. If hydroelectric production via turbines could be reduced or eliminated as a reservoir management objective by deploying floating PV on a small fraction of reservoir area, managers could focus on meeting alternate objectives, such as flood control and water supply.

Finally and most importantly, while we analyzed floating PV as an alternative to, and in reaction to deploying evaporation-based energy technology, a key point we would like to stress is that of PV space-efficiency. While PV deployment may have a vast potential on reservoirs and lakes, it is far from the only deployment option for this technology. As an example, Fig. 10 illustrates recent work we completed as part of the Minnesota Solar Pathway study [30]. The space needed to firmly generate 100% of the State of Minnesota's electricity with PV at lowest cost (i.e., including appropriate oversizing), is contrasted to the state's land cover[54]. This shows that open water is but one among many possibilities for PV deployment and that small, fractional deployments in any combination of land cover categories (in particular, already-perturbed high and medium intensity urban spaces) would be sufficient.

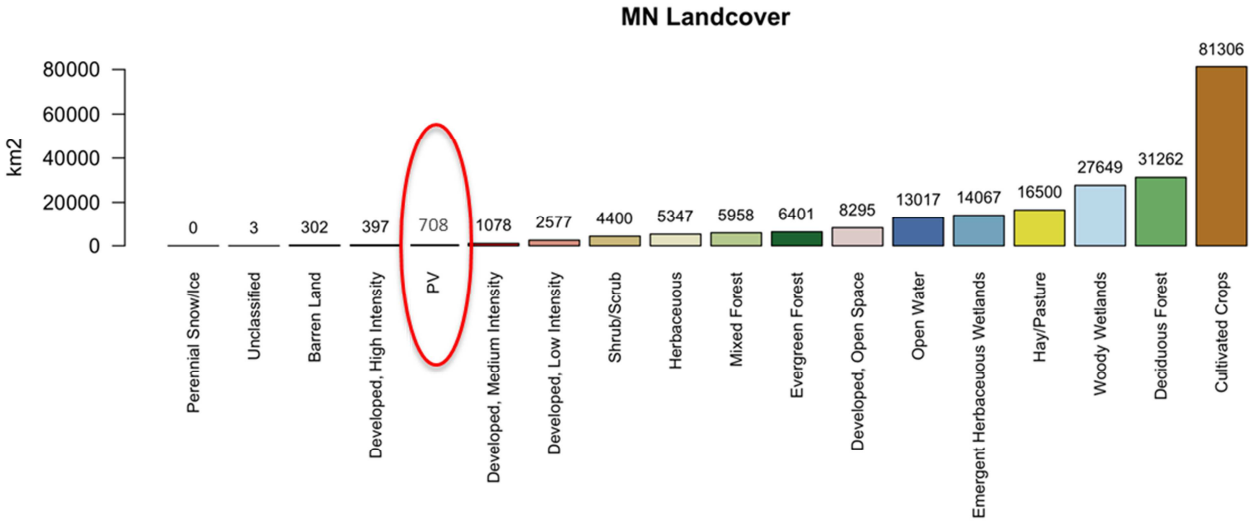

Figure 10: PV land requirement to firmly meet 100% of Minnesota's electricity demand, relative to the State's current land cover composition[54].

ACKNOWLEDGEMENTS

C.R.F. acknowledges funding from NASA award no. NNX16AM13G and NSF award no. AGS-1638936. OpenIFS was run under an educational software license with ECMWF. Mark Beauharnois created the standalone HTESSEL/FLAKE code framework used in this study. M.P acknowledges that some of the ideas and figures presented in the paper were developed as part of the Minnesota Solar Pathways project, a U.S. Department of Energy SunShot Initiative.

AUTHOR CONTRIBUTIONS

M. P. originated idea for this paper, performed PV simulations and led paper writing

R. P. synthesized PV, hydro, and evaporation results and co-wrote the paper

C.R.F. performed the lake water evaporation estimates and co-wrote the paper.

J. S. prepared lake-specific irradiance, temperature and wind speed data for PV and evaporation simulations

REFERENCES

1. Cavusoglu A.H., X. Chen, P. Gentile and O. Shin, (2017): Potential for natural evaporation as a reliable renewable energy resource. Nature Communications 8:617. DOI: 10.1038/s41467-017-00581-w |
2. Herkewitz, W., (2015): Here Is the World's First Engine Driven by Nothing But Evaporation. Popular Mechanics. http://www.popularmechanics.com/science/energy/a16045/evaporation-engine/ June 2015.
3. Ma, M., Guo, L., Anderson, D. G. & Langer, R. Bio-inspired polymer composite actuator and generator driven by water gradients. Science 339, 186–189 (2013).
4. Chen, X., Mahadevan, L., Driks, A. & Sahin, O. Bacillus spores as building blocks for stimuli-responsive materials and nanogenerators. Nat. Nanotechnol. 9, 137–141 (2014).
5. Zhang, L., Liang, H., Jacob, J. & Naumov, P. Photogated humidity-driven motility. Nat. Commun. 6, 7429 (2015).
6. Arazoe, H. et al. An autonomous actuator driven by fluctuations in ambient humidity. Nat. Mater. 15, 1084–1089 (2016).
7. Chen, X. et al. Scaling up nanoscale water-driven energy conversion into evaporation-driven engines and generators. Nat. Commun. 6, 7346 (2015).
8. Kim, S. H. et al. Bio-inspired, moisture-powered hybrid carbon nanotube yarn muscles. Sci. Rep. 6, 23016 (2016).
9. Ni, G. et al. Steam generation under one sun enabled by a floating structure with thermal concentration. Nat. Energy 1, 16126 (2016).
10. Xue, G. et al. Water-evaporation-induced electricity with nanostructured carbon materials. Nat. Nanotechnol. 12, 317–321 (2017).
11. US Energy Information Admisnistration, (2017): Electric Power Monthly. December 22, 2017 Issue.
12. EIA, Electric Power Annual 2016, December 2017, US Energy Information Administration, US Department of Energy, Washington, DC 20585. (https://www.eia.gov/electricity/annual/pdf/epa.pdf)
13. Minnesota Department of Commerce (2018) Minnesota Solar Pathways – Illuminating Pathways to 10% Solar: DoE SunShot grant under the Solar Energy Evolution and Diffusion Studies 2 – State Energy Strategies (SEEDS2-SES) program.
14. Cousins PJ, Smith DD, Luan HC, Manning J, Dennis TD, Waldhauer A, Wilson KE, Harley G, Mulligan WP. Generation 3: Improved performance at lower cost. Proc. Photovoltaics Specialist Conf., San Diego; 2010, pp. 275-8.
15. E.g., Dunlap, M., W. Marion, S. Wilcox, (1994): Solar radiation data manual for flat-plate and concentrating collectors. NREL/TP-463-5607. National Renewable Laboratory, Golden, CO.

16. ASTM E2848 - 13 Standard Test Method for Reporting Photovoltaic Non-Concentrator System Performance
17. Solarplaza Newsletter, 2018: Top 70 Floating Solar PV Plants. https://www.solarplaza.com/channels/top-10s/11761/top-70-floating-solar-pv-plants/
18. Trapani K. and Redón Santafé M. (2015), A review of floating photovoltaic installations: 2007–2013. Prog. Photovolt: Res. Appl., 23: 524–532. doi: 10.1002/pip.2466
19. Alok Sahu, Neha Yadav, K. Sudhakar, Floating photovoltaic power plant: A review, In Renewable and Sustainable Energy Reviews, Volume 66, 2016, Pages 815-824, ISSN 1364-0321, https://doi.org/10.1016/j.rser.2016.08.051.
20. Cazzaniga et al (2018) Floating photovoltaic plants: Performance analysis and design solutions. Renewable and Sustainable Energy Reviews 81. pp. 1730-1741
21. M. Rosa-Clot, Tina, G.M & Nizetic, S. (2017) Floating Photovoltaic Plants and Wastewater Basins: an Australian Project. Energy Procedia 134 pp 664-674. 9th International Conference on Sustainability in Energy and Buildings, SEB-17, 5-7 July 2017, Chania, Crete, Greece
22. Ferrer-Gisbert, C. et al (2013) A new Photovoltaic Floating Cover System for Water Reservoirs. Renewable Energy 60 pp.63-70
23. Liang, J. , Liang, J. (2017) Analysis and Modeling for China's Electricity Demand Forecasting Based on a New Mathematical Hybrid Method. Information 2017, 8, 33; doi; 10.3390/info8010033
24. Liu L. et al. (2017) Power Generation Efficiency and Prospects of Floating Photovoltaic Systems. Energy Procedia 105 pp.1136-1142. The 8th International Conference on Applied Energy – ICAE2016
25. NREL,(2017): National Solar Resource Data Base (NSRDB). https://nsrdb.nrel.gov/
26. Ong, S., Campbell, C., Denholm, P., Margolis, R. & Heath, G. Land-Use Requirements for Solar Power Plants in the United States. Report No. NREL/TP-6A20-56290, 47 (2013).
27. Perez, M. J. R. (2014). A model for optimizing the combination of solar electricity generation, supply curtailment, transmission and storage. (Order No. 3621033, Columbia University). ProQuest Dissertations and Theses, 246 pages
28. M. Perez, "Geographic Dispersion and Curtailment of VLS-PV Electricity," IEA PVPS Task 8 report, Ch.4 Future Technical Options for the Entire Energy System., 2015.
29. Perez, M., R. Perez, K. Rabago & M. Putnam, (2018): Lowest-Cost, Firm PV Without Conventional Backup: Supply Shaping Through Curtailment. Proc. (oral) IEEE PV Specialists Conference (WCPEC-7), Waikola, HI.
30. Minnesota Department of commerce (June 30th, 2018). Final Report Minnesota Solar Pathways Project, US Dept. of Energy Sunshot Contract No. DE-EE0007669
31. NREL (National Renewable Energy Laboratory) (2016): 2016 Annual Technology Baseline. Golden, CO: National Renewable Energy Laboratory. http://www.nrel.gov/analysis/data_tech_baseline.html.
32. Solaranywhere -- https://www.solaranywhere.com/
33. Perez, R., P. Ineichen, K. Moore, M. Kmiecik, C. Chain, R. George and F. Vignola, "A New Operational Satellite-to-Irradiance Model," Solar Energy vol. 73, no. 5, pp. 307-317, 2002
34. Menicucci, D.F., 1986, PVFORM Version 3. 2: a PV simulation program for mini and micro computer systems. Second version. National conference on microcomputer applications for renewable energy, Honolulu, HI, USA, 3 Mar 1987

35. Marion, W.; Anderberg, M. (2000). PVWATTS - An Online Performance Calculator for Grid-Connected PV Systems. Proceedings of the ASES Solar Conference, June 15-21, 2000, Madison, Wisconsin.
36. Perez, R., J. Schlemmer, A. Kankiewicz, J. Dise, A. Tadese, & T. Hoff, (2017): Detecting Calibration Drift at Ground Truth Stations. A Demonstration of Satellite Irradiance Models' Accuracy. In 43th IEEE PV Specialists Conference, 2017
37. E.g., M. A. Sanz-Bobi (ed.), Use, Operation and Maintenance of Renewable Energy Systems, Green Energy and Technology, DOI: 10.1007/978-3-319-03224-5_2, © Springer International Publishing Switzerland 2014
38. ECMWF. 2016. IFS documentation CY43R1: IV Physical Processes. Online at: https://www.ecmwf.int/search/elibrary/part?title=part&secondary_title=43R1
39. Mironov, D., E. Heise, E. Kourzeneva, B. Ritter, N. Schneider, and A. Terzhevik, 2010: Implementation of the lake parameterisation scheme FLake into the numerical weather prediction model COSMO. *Boreal Environ Res*, **15,** 218-230.
40. Stepanenko, V. M., S. Goyette, A. Martynov, M. Perroud, X. Fang, and D. Mironov, 2010: First steps of a Lake Model Intercomparison Project: LakeMIP. *Boreal Environ Res*, **15,** 191-202.
41. Balsamo, G., and Coauthors, 2015: ERA-Interim/Land: a global land surface reanalysis data set. Hydrol *Earth Syst Sc*, **19,** 389-407.
42. Choulga, M., E. Kourzeneva, E. Zakharova, and A. Doganovsky, 2014: Estimation of the mean depth of boreal lakes for use in numerical weather prediction and climate modelling. *Tellus Series a-Dynamic Meteorology and Oceanography*, **66**.
43. pers. comm. Margarita Choulga, Russian State Hydrometeorological University, 14 September 2017
44. Pan, M., X. Cai, N. W. Chaney, D. Entekhabi, and E. F. Wood (2016), An initial assessment of SMAP soil moisture retrievals using high-resolution model simulations and in situ observations, Geophys. Res. Lett., 43, 9662–9668, doi:10.1002/2016GL069964.
45. Pinker, R. T., and Coauthors, 2003: Surface radiation budgets in support of the GEWEX Continental-Scale International Project (GCIP) and the GEWEX Americas Prediction Project (GAPP), including the North American Land Data Assimilation System (NLDAS) Project. *J Geophys Res-Atmos*, **108**.
46. Xia, Y. L., and Coauthors, 2012a: Continental-scale water and energy flux analysis and validation for North American Land Data Assimilation System project phase 2 (NLDAS-2): 2. Validation of model-simulated streamflow. *J Geophys Res-Atmos*, **117**.
47. Xia, Y. L., and Coauthors, 2012b: Continental-scale water and energy flux analysis and validation for the North American Land Data Assimilation System project phase 2 (NLDAS-2): 1. Intercomparison and application of model products. *J Geophys Res-Atmos*, **117**.
48. Mesinger, F., and Coauthors, 2006: North American regional reanalysis. *B Am Meteorol Soc*, **87,** 343+
49. Cosgrove, B. A., and Coauthors, 2003: Real-time and retrospective forcing in the North American Land Data Assimilation System (NLDAS) project. *J Geophys Res-Atmos*, **108**.
50. Zhao, G., H. Gao, B. S. Naz, S.-C. Kao, and N. Voisin, Integrating a reservoir regulation scheme into a spatially distributed hydrological model, Advances in Water Resources, 98, 16-31, 2016.
51. Penman, H. L. (1948). Natural evaporation from open water, bare soil and grass. Proceedings of the Royal Society of London Series a-Mathematical and Physical Sciences, 193, 120-&.
52. Monteith, J. L. (1964). Evaporation and environment. The state of movement of water in living organisms. Symposium of the society of experimental biology (pp. 205−234).

53. Frempong, E., 1983, Diel aspects of the thermal structure and energy budget of a small English lake. Freshwater Biology, 13, pp. 89–102.
54. Multi-Resolution Land Characteristics Consortium: NLCD 2006 Land Cover (2011 Edition).
55. https://en.wikipedia.org/wiki/List_of_largest_reservoirs_in_the_United_States

APPENDIX

Table A1. Supplemental data for the 128 reservoir sample including physical properties[55] and 2006-2015 based estimates of aridity index, evaporation, hydroelectric capacity, and PV capacity.

Name	State(s)	Latitude (°)	Longitude (°)	Max Water Storage (km^3)	Surface Area at Capacity (km^2)	Depth at Capacity (m)	Regional Aridity Index	FLake *E* ($m\ yr^{-1}$)	Existing Peak Hydro Capacity (MW)	Mean PV Capacity (MW)
Abiquiu Lake	NM	36.28	-106.48	1.471	50.3	29	0.32	1.14	17	2,294
Alamo Lake	AZ	34.30	-113.55	1.287	69	19	0.11	1.60		3,209
Allegheny Reservoir	NY/PA	41.96	-78.93	1.604	85.7	19	1.41	0.84	400	2,705
American Falls Reservoir	ID	42.91	-112.75	2.063	230	9	0.30	0.94	112	9,052
Amistad Reservoir	COA/TX	29.47	-101.10	6.98	263	27	0.22	1.76	132	10,353
Arkabutla Lake	MS	34.74	-90.10	1.707	120	14	1.05	1.36		4,392
Banks Lake	WA	47.80	-119.20	1.573	109	14	0.28	0.96		3,698
Beaver Lake	AR	36.35	-93.92	2.405	128	19	1.08	1.20	112	4,716
Belton Lake	TX	31.13	-97.51	2.315	151.1	15	0.62	1.64		5,866
Bighorn Lake	MT / WY	45.11	-108.19	1.704	70	24	0.37	0.97	250	2,588
Broken Bow Lake	OK	34.21	-94.68	1.688	73	23	1.13	1.35		2,671
Brownlee Reservoir	ID/OR	44.59	-117.13	1.76	61	29	0.57	1.03	585	2,299
Bull Shoals Lake	AR/MO	36.50	-92.77	7.105	288.3	25	1.00	1.19	380	10,543
Canyon Ferry Lake	MT	46.52	-111.57	2.464	142.37	17	0.38	0.94	50	4,832
Cedar Creek Reservoir	TX	32.27	-96.14	1.338	140	10	0.77	1.52		5,372
Center Hill Lake	TN	36.03	-85.75	2.58	73.7	35	1.32	1.12	160	2,604
Cherokee	TN	36.27	-83.37	1.901	116.5	16	1.02	1.13	136	4,228

Lake										
Dale Hollow Reservoir	KY/TN	36.61	-85.31	2.104	112	19	1.30	1.14	54	3,903
DeGray Lake	AR	34.24	-93.19	1.699	73	23	1.21	1.34	68	2,665
Don Pedro Reservoir	CA	37.78	-120.36	2.504	52.4	48	0.45	1.41	203	2,209
Douglas Lake	TN	35.99	-83.37	1.802	115	16	1.08	1.20	146	4,133
Dworshak Reservoir	ID	46.61	-116.11	4.28	66.44	64	1.03	0.84	400	2,205
Elephant Butte Lake	NM	33.31	-107.17	2.547	145.62	17	0.19	1.43	28	6,992
Enid Lake	MS	34.15	-89.81	1.497	110	14	1.16	1.34	5	4,067
Eufaula Lake	OK	35.29	-95.54	4.685	420	11	0.99	1.31	90	15,733
F.D. Roosevelt Lake	WA	48.33	-118.17	11.795	320	37	0.53	0.93	6,900	10,280
Falcon Lake	TAM/TX	26.74	-99.23	3.263	354	9	0.24	1.85	63	14,021
Falls Lake	NC	36.02	-78.71	1.259	50.2	25	1.02	1.26		1,868
Flaming Gorge Reservoir	UT/WY	41.09	-109.54	4.673	170	27	0.25	0.77	152	6,942
Flathead Lake	MT	47.90	-114.10	1.501	510	3	1.28	0.80	208	15,943
Fontana Lake	NC	35.44	-83.68	1.78	41.4	43	1.34	1.05	239	1,513
Fort Gibson Lake	OK	35.95	-95.27	1.594	81	20	0.99	1.33	48	3,006
Fort Peck Lake	MT	47.76	-106.72	23.56	990	24	0.42	0.84	185	33,385
Grand Lake o' the Cherokees	OK	36.61	-94.85	2.062	188	11	1.05	1.26	120	6,992
Greers Ferry Lake	AR	35.52	-92.12	3.508	164	21	1.25	1.29	48	5,984
Grenada Lake	MS	33.83	-89.73	3.358	145	23	1.24	1.36	9	5,390
Guntersville Lake	AL	34.51	-86.16	1.257	275	5	1.18	1.26	496	10,034
Hugo Lake	OK	34.06	-95.42	1.572	141.82	11	0.95	1.38		5,300
Hungry Horse Reservoir	MT	48.23	-113.80	4.277	96.37	44	1.45	0.90	428	3,076
John H. Kerr Reservoir	NC/VA	36.57	-78.49	4.149	337	12	1.03	1.24	227	12,500
Jordan Lake	NC	35.74	-79.03	2.031	129	16	1.00	1.28	16	4,822
Kaw Lake	OK	36.77	-96.83	1.32	150	9	0.76	1.36	36	5,739

Kentucky Lake	KY/TN	36.52	-88.04	7.56	649	12	1.24	1.20	184	23,031
Keystone Lake	OK	36.23	-96.30	2.143	219.8	10	0.85	1.33	70	8,358
Lake Almanor	CA	40.26	-121.17	1.613	114	14	0.74	1.07	41	4,765
Lake Barkley	KY/TN	36.87	-87.99	2.568	234.4	11	1.22	1.20	130	8,271
Lake Berryessa	CA	38.59	-122.23	1.976	84	24	0.60	1.33	12	3,526
Lake Cumberland	KY	36.92	-85.02	7.511	265.2	28	1.21	1.08	270	9,193
Lake Elwell	MT	48.35	-111.25	1.869	60.06	31	0.36	0.76		2,062
Lake Francis Case	SD	43.44	-99.21	7.031	410	17	0.60	1.00	320	14,552
Lake Hartwell	GA/SC	34.50	-82.82	4.242	226.4	19	1.04	1.32	421	8,670
Lake Jocassee	NC/SC	34.98	-82.94	1.462	30.61	48	1.42	1.26	710	1,143
Lake Kemp	TX	33.76	-99.15	1.283	67.3	19	0.48	1.56		2,724
Lake Koocanusa	BC/MT	48.82	-115.28	7.24	189	38	0.99	0.81	600	6,113
Lake Lanier	GA	34.24	-83.95	3.15	190.94	16	1.14	1.28	130	7,181
Lake Livingston	TX	30.74	-95.13	2.634	370	7	0.82	1.50	24	14,051
Lake Marion	SC	33.46	-80.33	1.517	450	3	0.97	1.39		17,349
Lake Martin	AL	32.86	-85.89	2.001	180	11	1.01	1.35	182	6,847
Lake McClure	CA	37.64	-120.28	1.273	28.92	44	0.40	1.38	95	1,227
Lake McConaughy	NE	41.26	-101.84	2.146	144	15	0.49	1.06	52	5,503
Lake Mead	AZ/NV	36.14	-114.43	35.703	650	55	0.07	1.58	2,080	28,568
Lake Meredith	TX	35.64	-101.66	3.003	87.6	34	0.35	1.43		3,755
Lake Mohave	AZ/NV	35.41	-114.64	2.243	107	21	0.10	1.73	251	4,695
Lake Moultrie	SC	33.31	-80.06	1.369	240	6	0.97	1.38		9,324
Lake Murray	SC	34.06	-81.37	2.714	200	14	0.92	1.37	207	7,670
Lake Norman	NC	35.53	-80.94	1.349	131.6	10	1.02	1.28	350	4,979
Lake Oahe	ND/SD	45.30	-100.30	28.987	1500	19	0.53	0.92	786	52,215
Lake of the Ozarks	MO	38.16	-92.80	2.455	220	11	1.15	1.16	176	7,955
Lake Oroville	CA	39.57	-121.46	4.364	63.96	68	0.81	1.28	819	2,597
Lake Ouachita	AR	34.60	-93.32	3.414	195	18	1.20	1.31	75	7,180
Lake Pend Oreille	ID	48.15	-116.38	1.422	383	4	1.35	0.81	42	12,028

Lake Pleasant	AZ	33.89	-112.28	1.367	48.7	28	0.15	1.72	45	2,217
Lake Powell	AZ/UT	37.32	-110.79	32.336	660	49	0.18	1.25	1,320	29,590
Lake Ray Roberts	TX	33.41	-97.03	2.383	118.8	20	0.69	1.52		4,675
Lake Red Rock	IA	41.43	-93.16	1.771	260.9	7	1.10	0.97	36	9,031
Lake Sakakawea	ND	47.77	-102.29	29.974	1550	19	0.52	0.78	583	52,268
Lake Sharpe	SD	44.19	-99.68	2.356	230.2	10	0.57	0.94	493	8,172
Lake Strom Thurmond	GA/SC	33.81	-82.32	4.712	288	16	0.89	1.39	380	11,003
Lake Tawakoni	TX	32.81	-95.92	2.048	145	14	0.85	1.47		5,547
Lake Texoma	OK/TX	33.91	-96.65	6.164	360	17	0.77	1.43	80	13,979
Lake Travis	TX	30.41	-97.99	1.4	78.09	18	0.56	1.59	102	3,029
Lake Umatilla	OR/WA	45.79	-120.06	3.121	220	14	0.26	1.15	2,160	8,038
Lake Wallula	OR/WA	46.06	-118.94	1.665	157	11	0.29	1.11	1,127	5,471
Lake Winnibigoshish	MN	47.44	-94.19	1.322	274	5	0.67	0.78		9,002
Leech Lake	MN	47.16	-94.41	1.233	416.62	3	0.76	0.79		13,863
Lewis Smith Lake	AL	33.96	-87.11	1.715	86	20	1.26	1.27	157	3,167
Lewisville Lake	TX	33.11	-96.97	2.569	93.2	28	0.69	1.53		3,643
Mark Twain Lake	MO	39.65	-91.75	2.594	215	12	1.16	1.06	58	7,612
Milford Lake	KS	39.16	-96.92	1.388	130	11	0.83	1.18		4,910
Millwood Lake	AR	33.75	-93.98	2.288	385	6	0.99	1.37		14,343
Navajo Lake	CO/NM	36.90	-107.46	2.108	63.2	33	0.29	1.09	32	2,916
New Melones Lake	CA	37.99	-120.53	2.985	51	59	0.46	1.31	300	2,141
Norfork Lake	AR/MO	36.36	-92.23	2.446	89	27	1.09	1.20		3,267
Norris Lake	TN	36.29	-83.92	2.516	138	18	1.25	1.16	132	4,897
Oologah Lake	OK	35.55	-95.60	1.874	230	8	0.98	1.31	132	8,657
Owyhee Reservoir	OR	43.46	-117.34	1.46	55	27	0.27	1.04	12	2,074
Painted Rock Reservoir	AZ	33.03	-112.87	3.073	215	14	0.09	1.64		9,907
Palisades Reservoir	ID/WY	43.24	-111.12	1.728	65	27	0.75	0.84	177	2,480

Pathfinder Reservoir	WY	42.42	-106.91	1.254	89	14	0.28	0.91	67	3,580
Perry Lake	KS	39.18	-95.46	1.749	102.75	17	0.93	1.13		3,731
Pine Flat Lake	CA	36.86	-119.30	1.233	24.2	51	0.42	1.24	165	1,034
Quabbin Reservoir	MA	42.36	-72.30	1.571	99.27	16	1.53	0.89		3,241
Red Lake Reservoir	MN	48.07	-95.03	4.228	1168.1	4	0.54	0.78	5	38,866
Richard B. Russell Lake	GA/SC	34.09	-82.64	1.836	107.8	17	0.96	1.36	600	4,117
Richland-Chambers Reservoir	TX	31.98	-96.19	2.15	181.1	12	0.74	1.53		6,916
Riffe Lake	WA	46.48	-122.29	2.078	47.9	43	2.55	0.79	300	1,341
Ross Lake	BC/WA	48.85	-121.03	1.77	47	38	2.10	0.79	460	1,339
Sam Rayburn Reservoir	TX	31.21	-94.28	4.931	463	11	0.92	1.47	25	17,547
San Luis Reservoir	CA	37.06	-121.12	2.518	51	49	0.17	1.36	424	2,190
Sardis Lake	MS	34.49	-89.64	1.865	237	8	1.13	1.33	15	8,738
Seminoe Reservoir	WY	42.04	-106.85	1.255	82.11	15	0.27	0.85	45	3,323
Shasta Lake	CA	40.77	-122.30	5.615	120.4	47	1.05	1.23	676	4,809
Smith Mountain Lake	VA	37.08	-79.62	2.837	83	34	1.03	1.19	560	3,047
Stockton Lake	MO	37.61	-93.77	2.065	256	8	1.19	1.19	52	9,267
Strawberry Reservoir	UT	40.17	-111.13	1.365	69.46	20	0.55	0.68	45	2,913
Table Rock Lake	AR/MO	36.62	-93.41	4.27	212	20	1.07	1.20	200	7,775
Tenkiller Ferry Lake	OK	35.67	-94.98	1.518	84	18	1.01	1.27	34	3,128
Theodore Roosevelt Lake	AZ	33.68	-111.11	3.59	129	28	0.26	1.59	36	5,982
Toledo Bend Reservoir	LA/TX	31.49	-93.73	5.517	735	8	0.94	1.50	92	27,716
Trinity Lake	CA	40.88	-122.71	3.019	66.91	45	1.21	1.11	140	2,704
Truman Reservoir	MO	38.26	-93.44	6.398	847	8	1.01	1.18	160	30,582
Tuttle Creek Lake	KS	39.35	-96.68	3.93	217.6	18	0.85	1.14		8,123
Wappapello Lake	MO	36.95	-90.31	1.4	94	15	1.24	1.21	3	3,386

Watts Bar Lake	TN	36.77	-84.67	1.449	160	9	1.30	1.10	190	5,539
Weiss Lake	AL	34.18	-85.60	1.768	122	14	1.07	1.27	30	4,524
Wheeler Lake	AL	34.71	-87.14	1.295	272	5	1.18	1.22	361	9,850
Whitney Lake	TX	32.85	-96.52	2.591	240	11	0.75	1.48	38	9,234
Wright Patman Lake	TX	33.27	-94.22	3.274	484	7	0.99	1.42		18,205